Molecular Biology of the Cell
Vol. 16, 4572–4583, October 2005

TOR Complex 2 Integrates Cell Movement during Chemotaxis and Signal Relay in *Dictyostelium*

Susan Lee,* Frank I. Comer,† Atsuo Sasaki,* Ian X. McLeod,‡ Yung Duong,* Koichi Okumura,§ John R. Yates III,‡ Carole A. Parent,† and Richard A. Firtel*

*Section of Cell and Developmental Biology, Division of Biological Sciences and Center for Molecular Genetics, University of California, San Diego, La Jolla, CA 92093-0380; †Laboratory of Cellular and Molecular Biology, Division of Basic Sciences, NCI/National Institutes of Health, Bethesda, MD 20892-4256; ‡Department of Cell Biology, Scripps Research Institute, La Jolla, CA 92037; and §Ludwig Institute for Cancer Research, School of Medicine, University of California, San Diego, La Jolla, CA 92093-0660

Submitted April 25, 2005; Revised July 8, 2005; Accepted July 21, 2005
Monitoring Editor: Anne Ridley

Dictyostelium **cells form a multicellular organism through the aggregation of independent cells. This process requires both chemotaxis and signal relay in which the chemoattractant cAMP activates adenylyl cyclase through the G protein-coupled cAMP receptor cAR1. cAMP is produced and secreted and it activates receptors on neighboring cells, thereby relaying the chemoattractant signal to distant cells. Using coimmunoprecipitation and mass spectrometric analyses, we have identified a TOR-containing complex in *Dictyostelium* that is related to the TORC2 complex of *Saccharomyces cerevisiae* and regulates both chemotaxis and signal relay. We demonstrate that mutations in *Dictyostelium* LST8, RIP3, and Pia, orthologues of the yeast TORC2 components LST8, AVO1, and AVO3, exhibit a common set of phenotypes including reduced cell polarity, chemotaxis speed and directionality, phosphorylation of Akt/PKB and the related PKBR1, and activation of adenylyl cyclase. Further, we provide evidence for a role of Ras in the regulation of TORC2. We propose that, through the regulation of chemotaxis and signal relay, TORC2 plays an essential role in controlling aggregation by coordinating the two essential arms of the developmental pathway that leads to multicellularity in *Dictyostelium*.**

INTRODUCTION

TOR, Target of rapamycin, is a member of the PI3K-related family of serine/threonine protein kinases and a known regulator of cell growth in eukaryotic cells (Lorberg and Hall, 2004). The protein complex that controls this pathway, termed TOR Complex 1 (TORC1), is highly conserved in evolution and contains the conserved proteins LST8 and KOG1/Raptor complexed with TOR (Loewith *et al.,* 2002; Jacinto *et al.,* 2003; Hay and Sonenberg, 2004). In addition, TOR controls other pathways, including regulated polarized actin assembly in *S. cerevisiae* (Schmidt *et al.,* 1996). A distinct TOR complex, TORC2, contains TOR, LST8, and three other proteins: AVO1, AVO2, and AVO3. TORC2 regulates this cytoskeletal rearrangement (Loewith *et al.,* 2002), and a related TORC2 has been identified in mammalian cells that contains, in addition to TOR and LST8, the AVO3 ortholog mAVO3/Rictor (Jacinto *et al.,* 2004; Sarbassov dos *et al.,* 2004). AVO1 and AVO3 are orthologues of two previously identified *Dictyostelium* proteins, RIP3 (Ras interacting protein 3) and Pia (Pianissimo) (Chen *et al.,* 1997; Lee *et al.,* 1999). Disruption of either of these gene products in *Dictyostelium* (*pia* null [*pia*$^-$] and *rip3* null [*rip3*$^-$] cells) gives rise to serious developmental defects, because they are unable to activate the aggregation-stage adenylyl cyclase ACA in response to chemoattractant stimulation and are defective in chemotaxis.

In *Dictyostelium*, the activation of ACA and chemotaxis are closely integrated responses, although they have been thought to be independently regulated (Comer *et al.,* 2005). On starvation, *Dictyostelium* cells initiate a developmental program that requires chemotaxis toward extracellular cAMP emitted by neighboring cells, which leads to the formation of multicellular aggregates (Parent and Devreotes, 1996; Aubry and Firtel, 1999; Kimmel and Parent, 2003). The chemoattractant cAMP binds to the heterotrimeric G-protein-coupled cAMP receptor cAR1, which activates multiple intracellular signaling events that control chemotaxis, the activation of adenylyl cyclase A (ACA), and gene expression required for aggregation (Aubry and Firtel, 1999; Kimmel and Parent, 2003). The activation of ACA produces more cAMP, which acts both intracellularly to activate protein kinase A (PKA) and mediated downstream effectors and extracellularly to initiate chemotaxis and to relay the chemoattractant signal to distal cells (signal relay). The concerted regulation of chemotaxis and signal relay comprises a system that efficiently culminates with the development of a true, differentiated multicellular organism. In this article, we demonstrate that *Dictyostelium* TORC2 functions as an integrator of multiple distinct signaling pathways to control aggregation and the formation of the multicellular organism. Cells lacking any of the TORC2 proteins LST8, RIP3 (AVO1), and Pia (AVO3, mAVO3, Rictor) exhibit strong chemotaxis defects including loss of speed, cell polarity, and directionality, and are unable to fully activate Akt/PKB and the related kinase PKBR1, both of which are required for cell polarity and chemotaxis and are defective

This article was published online ahead of print in *MBC in Press* (http://www.molbiolcell.org/cgi/doi/10.1091/mbc.E05–04–0342) on August 3, 2005.

Address correspondence to: Richard A. Firtel (rafirtel@ucsd.edu).

in their capacity to activate adenylyl cyclase in response to chemoattractant stimulation. Further, we demonstrate that RIP3 carrying a point mutation that abrogates Ras-GTP binding is unable to fully complement the null mutation, suggesting that Ras plays a role in mediating TORC2 function.

MATERIALS AND METHODS

Biochemical and Chemotaxis Assays

To obtain developmentally competent cells capable of responding to cAMP as a chemoattractant, log-phase vegetative cells were washed twice and resuspended at a density 5×10^6 cells/ml with 12 mM Na^+/K^+ phosphate buffer, pH 6.2, and pulsed with 30 nM cAMP for 5 h at 6-min intervals. Cells were then washed and resuspended in 12 mM Na^+/K^+ phosphate buffer.

The chemoattractant receptor-mediated activation of adenylyl cyclase was carried out as previously described (Parent and Devreotes, 1995). Briefly, differentiated cells were stimulated with 50 μM cAMP and filter lysed at the indicated time points into Tris buffer containing ^{32}P-αATP diluted with unlabeled ATP to a final concentration of ~150 Ci/mol. The reaction was allowed to proceed for 1 min, stopped with SDS/ATP, and the radiolabeled cAMP was purified by column chromatography. Adenylyl cyclase assays exhibit considerable variability between experiments. Although the relative extent of activation of different cell lines or treatment conditions is highly reproducible between experiments, the absolute activity can vary significantly (2–3-fold at times) from day to day. Therefore we, and others in the field, have chosen to present adenylyl cyclase activation data as representative of results from at least 3–5 independent experiments, each performed in duplicate on a given day. Furthermore, comparisons between different cell lines or treatment conditions are made on samples assayed on the same day.

For direct G-protein stimulation of adenylyl cyclase, differentiated cells were filter lysed with GTPγS (50 μM final concentration) and, after 5 min, adenylyl cyclase activity was assayed for 2 min. To prepare cytosolic extracts for the in vitro complementation experiments, cells were suspended at 8×10^7 cells/ml in simple lysis buffer (SLB, 10 mM Tris, pH 7.5, 0.2 mM EGTA, 200 mM sucrose), filter lysed, and centrifuged at $9500 \times g$ for 20 min. The in vitro complementation was performed in essentially the same manner as the direct GTP-γ-S-stimulated adenylyl cyclase activation assay, except that cells were lysed directly into cytosolic extract.

The PKB and PKBR1 kinase activities were assayed as described previously (Meili *et al.,* 1999, 2000). Briefly, unstimulated differentiated cells (0 time point) and differentiated cells stimulated with cAMP for various times were lysed with an equal volume of 2× NP-40 lysis buffer (2× phosphate-buffered saline, 100 mM NaF, 2% NP-40, 4 mM EDTA, 2 mM pyrophosphate, 2 mM Na_3VO_4, and protease inhibitors leupeptin and aprotinin) on ice for 10 min. The lysate was precleared by centrifugation for 10 min. To immunoprecipitate PKB or PKBR1, the anti-PKB or anti-PKBR1 antibody and 30 μl of slurry of protein A-Sepharose were added into the supernatant. The beads were washed twice with lysis buffer and twice with kinase buffer (25 mM MOPS, pH 7.4, 25 mM β-glycerophosphate, 20 mM $MgCl_2$, and 1 mM dithiothreitol [DTT]). We incubated beads with 75 μl of kinase buffer containing 5 μM cold ATP, 10 μCi of γ-^{32}P-ATP, and 5 μg of H2B as substrate at room temperature for 15 min. The reaction was stopped by the addition of 25 μl of 5× sample buffer (250 mM Tris, 500 mM DTT, 10% SDS, 50% glycerol, and 0.5% bromophenol blue) and boiled for 2 min. Samples were separated by 12% SDS-PAGE, blotted onto a polyvinylidene difluoride (PVDF) membrane, and exposed to film. After the autoradiography, the lower part of the membrane containing the phosphorylated H2B was cut off and the upper portion with the Akt/PKB or PKBR1 was subjected to Western blot analysis to quantify the level of Akt/PKB or PKBR1 in each lane. Experiments were repeated independently at least three times, always assaying wild-type cells as a control for comparison in each experiment. The wild-type samples were run on the same gel as one of the experimental strains, and all gels and membranes were coprocessed together.

Ras activation was performed as previously described (Sasaki *et al.,* 2004). F-actin polymerization and myosin II assembly were assayed as described previously (Lee *et al.,* 2004; Park *et al.,* 2004). Experiments were repeated independently at least three times, always including a wild-type control for comparison.

Chemotaxis analysis was performed as described previously (Park *et al.,* 2004; Sasaki *et al.,* 2004) and analyzed using DIAS software (Wessels *et al.,* 1998). Differentiated cells were plated in Na^+/K^+ phosphate buffer at a density of 6×10^4 cells/cm^2 onto a plate with a hole covered by a 0.17-mm glass coverslip. An Eppendorf Patchman micromanipulator with a glass capillary filled with 150 μM cAMP solution was brought into the field of view of an inverted microscope. The response of the cells was recorded by time-lapse video. Experiments were performed at least three times on different days, always including a wild-type control strain in the analyses.

Cell Growth in the Presence of Rapamycin

Cells growing in log phase (~3–4 $\times$ 10^6 cells/ml) were diluted to 4×10^5 cells/ml in HL5 medium. Rapamycin (Sigma Chemical Co, St. Louis, MO) was dissolved in dimethyl sulfoxide as a 1 mM stock and added to the cultures to the indicated concentration. Cell number in the suspension cultures was monitored over 4 d, with no further addition of the drug.

Translocation Assays

The chemoattractant-mediated recruitment of the CRAC PH domain (PH_{CRAC}-GFP) to the plasma membrane was measured biochemically as previously described in response to 20 μM cAMP (Parent *et al.,* 1998), except that protein samples were subjected to PAGE analysis using NuPage 4–12% Bis-Tris protein electrophoresis gradient gels, according to the manufacturer-recommended protocol (Invitrogen, Carlsbad, CA). For microscopic observation of translocation, cells expressing PH_{CRAC}-GFP were stimulated with 20 μM cAMP and fixed (1% formaldehyde, 0.125% glutaraldehyde, 0.01% Triton X-100 in PB) after 5 s of stimulation. Cells were viewed with an inverted Zeiss Axiovert S100 microscope (Thornwood, NY) equipped with automated filter wheels (Ludl Electronic Products, Hawthorne, NJ). Images were recorded with a CoolSnap HQ CCD camera (Roper Scientific, Trenton, NJ) operated by IPLab software (Scanalytics, Fairfax, VA). GFP-PhdA translocation was examined by real-time fluorescent video microscopy as described previously (Funamoto *et al.,* 2001).

Detection of the Dd-TOR Complex

Aggregation-competent cells were washed with Na/K phosphate buffer and resuspended at a density of 1×10^8 cells/ml in Na/K phosphate buffer containing 20 mM MOPS (pH 7.0) and 1 mM phenylmethylsulphonyl fluoride. Cells were mechanically lysed by filtration (Nuclepore Track Etch membrane, 3 μm; Whatman, Clifton, NJ). Subsequently, cell lysates were incubated in 2.5 mg/ml DSP (ditho-bis-succinimidylpropionate, Calbiochem, La Jolla, CA) for 5 min. The cross-linking reactions were quenched with 200 mM Tris-HCl (pH 7.4). A sample was mixed with an equal volume of 2× lysis buffer A (1% NP-40, 300 mM NaCl, 40 mM MOPS, pH 7.0, 20% glycerol, 2 mM Na_3VO_4, 2 μg/ml leupeptin, 5 μg/ml aprotinin) and centrifuged. Total cell extracts and immunoprecipitates with 25 μl resin of anti-V5 (V5–10) antibody agarose conjugate (Sigma) were analyzed by silver staining or immunoblotting with anti-T7 (Novagen, Madison, WI) and anti-V5 antibodies. For identifying the Dd-TOR complex, the anti-V5 antibody immunoprecipitated products were eluted with the buffer containing 4% SDS and 0.1 M glycine (pH 2.5). The protein complex was incubated with 100 mM DTT and then precipitated with methanol/chloroform.

Mass Spectrometry

The samples were washed with acetone, resuspended in Tris buffer, 8 M urea, pH 8.6, reduced with 100 mM TCEP, and alkylated with 55 mM iodoacetamide. Trypsin digest was done in the presence of 1 mM $CaCl_2$ for tryptic specificity. Peptide mixtures were loaded onto a triphasic LC/LC column with the following steps of 500 mM ammonium acetate bumps: 25, 35, 50, 80, and 100%. Tandem mass spectra were analyzed using DTA Select and the *Dictyostelium* sequence database with the following filtering parameters for cross correlation scores 1.8 (+1), 2.8 (+2), and 3.5 (+3) (Washburn *et al.,* 2001). Identities of specific bands were confirmed by sequence analysis.

Constructs

The LST8 knockout construct was made by inserting the blasticidin resistance (Sutoh, 1993) cassette into a *Bam*HI site created at nucleotide 500 of the LST8 genomic DNA sequence. A 5′-fragment was amplified from genomic DNA by PCR by using the primers GTTTTTGAATTCAGTTTTGATGGTCATAAAGGTAATG and GTTTTTGGATCCGGTCAATGATGTTATACC and subsequently digested with enzymes *Eco*RI and *Bam*HI. A 3′ fragment was amplified by using the primers GTTTTTGGATCCTCAAGTGATGGTGGTTTAG and GTTTTTCTCGAGTTTTTATCTTGGTAAATCATTTAAAGCAAC subsequently digested with *Bam*HI and *Xho*I. The vector was digested with *Eco*RI and *Xho*I and the DNA was transformed into *Dictyostelium* cells. The knockout clones were confirmed by Southern and Northern blot analysis. Two independent clones were picked and examined. Both showed the same chemotaxis defects described in the results.

A T7-tagged full length LST8 ORF (open reading frame) clone was amplified from genomic DNA by PCR using primers 5′- GTTTTTGAATTCAAAAAAATGGCTTCAATGACTGGTGGTCAACAAATGGGTCCAGGTATTATATTGGCAACAGCATC and GTTTTTCTCGAGTTTTTATCTTGGTAAATCATTTAAAGCAAC-3′ subsequently digested with *Eco*RI and *Xho*I and subcloned to expression vector Exp4(+).

A 3′ V5-tagged, full-length Pia clone was amplified from genomic DNA by PCR using primers GTTTTTGATATCAAAAAAATGACAAGTTCTGATAGTAGTG and GTTTTTCTCGAGTTTTTAAGTTGAATCTAAACCTAATAATGGATTTGGAATTGGTTTACCATTTAAATCATGATATGGATCAGATG and subsequently digested by *Eco*RV and *Xho*I and subcloned into the expression vector Exp4(+).

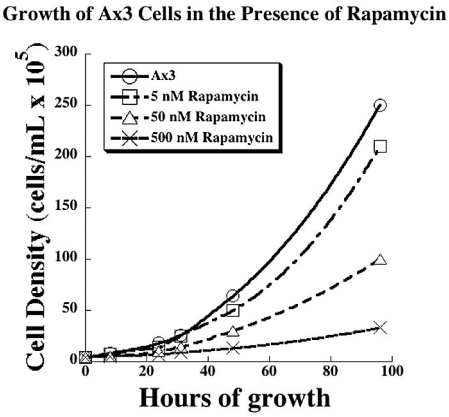

Figure 1. Inhibition of *Dictyostelium* cell growth by rapamycin. The increases in cell number of wild-type cells in the absence and presence of different concentrations of rapamycin are shown. See *Materials and Methods* for details.

A 5′ T7-tagged clone of RIP3 from ATG to internal *Bam*HI site at nucleotide 1490 was amplified by PCR from the full-length RIP3 (Lee *et al.*, 1999) by using primers GTTTTTGAATTCAAAAAAATGGCTTCAATGACTGGTGGTCA-ACAAATGGGTTCAGTTTATTGTGAATTAGTTGATG and ATTTGGACA-AAGTACCAATACTTC. The full length of 5′ T7-tagged RIP3 clone was obtained by digesting the PCR product with *Eco*RI and *Bam*HI and the full-length RIP3 with *Bam*HI and *Xho*I and the fragments cloned into the expression vector Exp4(+).

All constructs were sequenced.

RESULTS

Dictyostelium Expresses Orthologues of the Yeast and Mammalian TOR Complex 2

The previously identified *Dictyostelium* proteins RIP3 and Pia are orthologues of the TORC2 components AVO1 and AVO3/mAV03/Rictor in *S. cerevisiae* and mammals, respectively (Chen *et al.*, 1997; Lee *et al.*, 1999; Loewith *et al.*, 2002). Previous studies indicated that both *Dictyostelium* proteins are required for efficient chemotaxis and the activation of ACA to relay the cAMP signal to neighboring cells. The WD40-repeat protein LST8 is a known component of both yeast and mammalian TORC1 and TORC2. We identified a single gene in the *Dictyostelium* database (GenBank accession no. DDB0184464) that encodes an LST8 ortholog. We created an LST8 gene knockout by homologous recombination. The knockout strain (*lst8*$^-$ cells) was confirmed by Southern and RNA blot analyses (see *Materials and Methods*). Analysis of the *lst8*$^-$, *pia*$^-$, and *rip3*$^-$ cells showed that these cells were the same size and exhibited the same growth kinetics as the parental wild-type cells (unpublished data), indicating that these genes do not regulate *Dictyostelium* growth under the conditions tested (rich axenic medium containing 1% yeast extract, 1% proteose peptone, and 1% dextrose or in association with bacteria as a food source). Because RIP3, Pia, and LST8 are homologues of proteins complexed with TOR in yeast and mammalian cells, we examined whether rapamycin, which inhibits TORC1 but not TORC2 (Loewith *et al.*, 2002; Jacinto *et al.*, 2004), inhibits growth. Addition of rapamycin to concentrations of 50 nM dramatically inhibited cell growth, whereas 500 nM rapamycin resulted in an almost complete cessation of growth, consistent with the involvement of a rapamycin-sensitive TORC1 in controlling cell growth in *Dictyostelium* (Figure 1).

When plated for development on nonnutrient agar in the absence of exogenous pulses of cAMP, we found that, similar to *rip3*$^-$ and *pia*$^-$ cells, *lst8*$^-$ cells do not spontaneously aggregate, but remain as a smooth monolayer of cells (Figure 2A; Chen *et al.*, 1997; Lee *et al.*, 1999). When provided with exogenous pulses of cAMP, which mimic the endogenous cAMP signaling of wild-type cells, and then plated for development, *lst8*$^-$ and *pia*$^-$ cells still do not develop. In contrast, *rip3*$^-$ cells form mounds, although very inefficiently (Figure 2A; Lee *et al.*, 1999), suggesting that the *rip3*$^-$ defect can be partially overridden, a phenotype that is also shared with the Ras GEF (guanine nucleotide exchange factor) Aimless (Insall *et al.*, 1996; Lee *et al.*, 1999). Defects in the ability to aggregate can result in an inability to induce the genes required for this process.

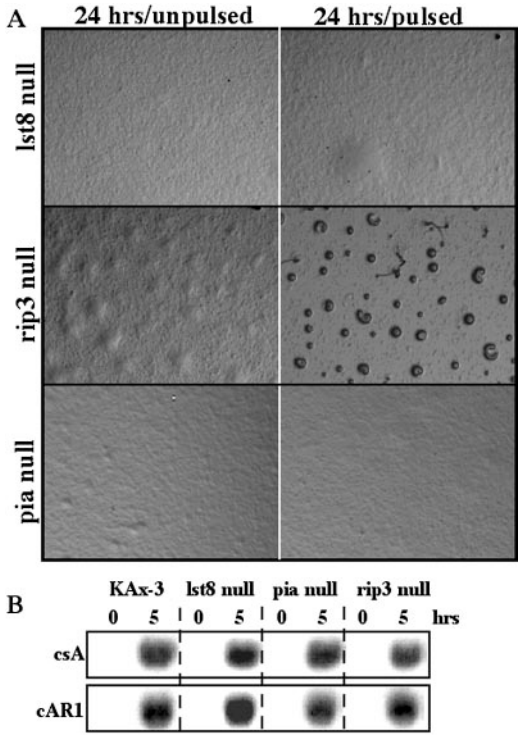

Figure 2. Development of *rip3*$^-$, *pia*$^-$, and *lst8*$^-$ cells. (A) Development of *rip3*$^-$, *pia*$^-$, and *lst8*$^-$ and wild-type cells plated on nonnutrient agar (left side). The cells in the right-hand panels were first pulsed for 6 h with 30 nM cAMP, to mimic the natural cAMP oscillations that induce aggregation-stage responses, before plating. All pictures were taken at 24 h. (B) RNA blot showing the expression of two pulse-induced genes (cAR1 and csA) at 0 time and after 5 h of cAMP pulsing.

To assess whether LST8, Pia, or RIP3 regulates the expression of early genes required for development, we performed an RNA blot analysis examining the expression of the cAMP receptor cAR1 and csA (gp80), a cell adhesion molecule, both of which are required for aggregation. We find that cAR1 and csA transcripts are normally induced in response to exogenous cAMP in *lst8*$^-$, *pia*$^-$, and *rip3*$^-$ cells (Figure 2B). These data suggest that the developmental defects of *lst8*$^-$ cells, like *rip3*$^-$ and *pia*$^-$ cells, may arise from deficiencies in chemotaxis and/or chemoattractant signal relay.

Dictyostelium TORC2 Exists in a Preformed Complex That Regulates Adenylyl Cyclase Activation

To investigate the underlying developmental defect of *lst8*$^-$ cells, we measured their capacity to activate ACA in response to chemoattractant stimulation. In this activation trap

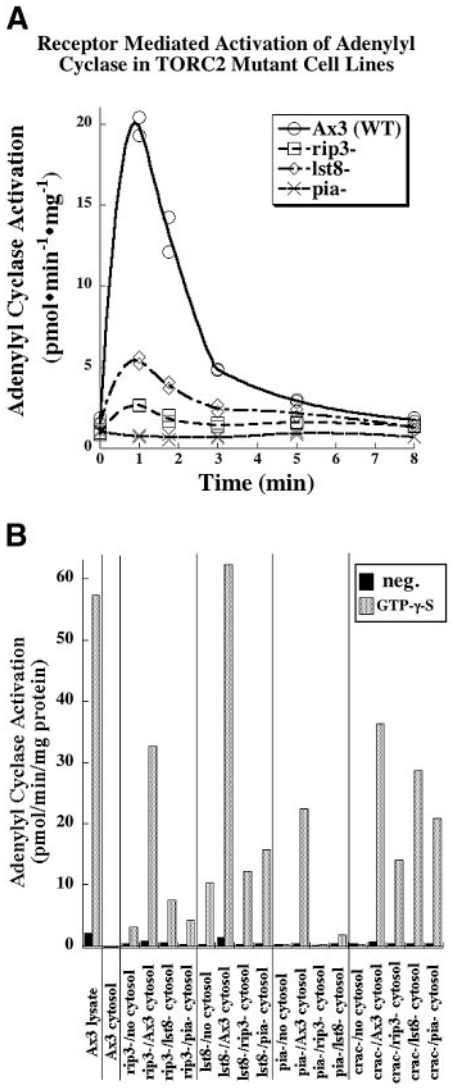

Figure 3. Receptor-mediated activation of adenylyl cyclase is impaired in TORC2 mutant cell lines. (A) Adenylyl cyclase activity of each of the indicated cell lines was measured as de novo synthesis of ^{32}P-labeled cAMP following the addition of the chemoattractant cAMP to a final concentration of 50 μM. Data are representative of results from 3 to 4 independent experiments, each performed in duplicate. (B) Cytosolic extracts of wild-type KAx-3 and each of the TORC2 mutant cell lines were prepared as described in the *Materials and Methods*. Direct G protein-mediated activation of adenylyl cyclase was measured after stimulation of cell lysates with GTPγS in the absence or presence of the indicated cytosolic extract. The data set for each combination is listed in the format: mutant cell lysate/cytosolic extract. The data presented are representative of three independent experiments, each performed in duplicate.

assay (Parent and Devreotes, 1995; Lee *et al.*, 1999), chemoattractant receptor-mediated ACA activation is measured by stimulating cells with a saturating dose of cAMP, rapidly lysing aliquots at specific time points, and determining the amount of new cAMP synthesis. Wild-type cells display a rapid rise in enzyme activity, peaking ~1 min after addition of chemoattractant, followed by a return to basal levels within 7–10 min. A representative experiment (see *Materials and Methods*) is shown in Figure 3A. Cells lacking LST8 are defective in this response, showing dramatically reduced ACA activation (Figure 3A). Parallel experiments on *rip3*$^-$ and *pia*$^-$ cells reveal a similar loss of receptor-stimulated ACA activity, consistent with previous findings (Figure 4A; Chen *et al.*, 1997; Lee *et al.*, 1999). We also found a similar defect in ACA activation in response to GTP-γ-S, which directly and constitutively activates G proteins downstream of chemoattractant receptors (Figure 3B). From these results, we conclude that LST8 must act downstream of G protein activation and that the developmental defect of *lst8*$^-$ cells is at least partially due to defective chemoattractant signal relay through ACA.

To gain more insight into the mechanisms by which components of TORC2 regulate ACA activity, we performed a series of in vitro reconstitution experiments. Previous work indicated that, in addition to receptor linked heterotrimeric G proteins, chemoattractant-mediated activation of ACA requires multiple cytosolic factors, including CRAC (cytosolic regulator of adenylyl cyclase), Pia, and RIP3 (Insall *et al.*, 1994; Chen *et al.*, 1997; Lee *et al.*, 1999). One can achieve in vitro complementation of CRAC null (*crac*$^-$) cells, thus restoring GTPγS-stimulated ACA activity, by combining a *crac*$^-$ cell lysate with cytosol derived from wild-type cells (Lilly and Devreotes, 1995). We have utilized this approach to further examine the activation of adenylyl cyclase in *rip3*$^-$, *pia*$^-$, and *lst8*$^-$ cells. We hypothesized that if these components exist in a stable, preformed complex, one may be able to reconstitute GTPγS-stimulated ACA activity with wild-type cytosol, but may not be able to cross-complement between different mutant strains. As depicted in Figure 3B, addition of wild-type cytosol to lysates from any of the putative TORC2 mutant or *crac*$^-$ cell lines results in strong reconstitution of GTPγS-stimulated ACA activity. Likewise, we found significant reconstitution of *crac*$^-$ cell lysates with cytosolic fractions from any of the TORC2-deficient cell lines, although the rescue is more modest with cytosol from *rip3*$^-$ cells than with cytosol from *pia*$^-$ or *lst8*$^-$ cells. In contrast, addition of cytosol from any of the TORC2 mutants to lysates from any of the other TORC2 mutants reconstitutes little or no GTPγS-stimulated ACA activity. These data support the hypothesis that RIP3, LST8, and Pia all function together in a preformed complex to promote ACA activation. Furthermore, our observations suggest that these preformed TORC2 complexes either cannot exchange components rapidly or are unstable in the absence of all of the subunits.

Dictyostelium TORC2 Components Form a Complex

Our data suggest that RIP3, Pia, and LST8 regulate common biochemical pathways. To examine whether these proteins are found in a complex, we coexpressed two different pairwise combinations of RIP3, LST8, and Pia harboring different epitope tags in wild-type cells and performed coimmunoprecipation experiments. Figure 4, A and B, show that T7-tagged RIP3 coimmunoprecipitates with V5-tagged Pia (V5-Pia) and that T7-tagged LST8 (T7-LST8) immunoprecipitates with V5-Pia, suggesting that they can form a TORC2-like complex in vivo.

To further characterize the components of such complexes, we used anti-V5 antibody cross-linked to Sepharose beads to purify Pia and associated proteins from cytosolic extracts of *Dictyostelium*. This purified sample was subjected to mass spectrometric (MS) analysis. Cytosolic extracts from untransformed cells were used as a control. The MS analysis showed that LST8 and TOR associate with V5-Pia (Figure 3C). 14-3-3, and heat shock proteins were preferentially found in the experimental but not the control sample. Although *Dictyostelium* encodes a Raptor/KOG1 ortholog

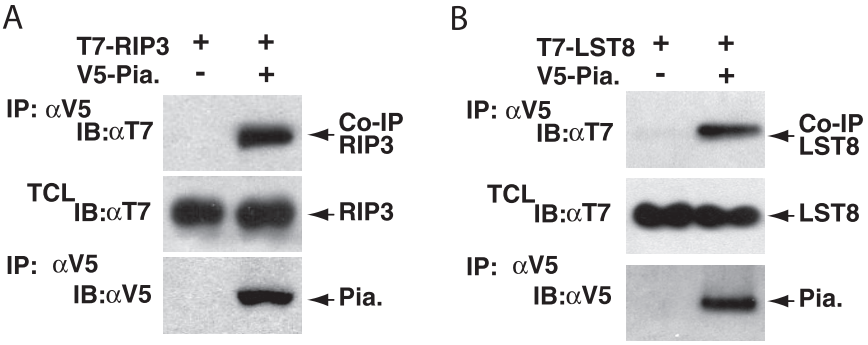

C

Locus	DDB0217978	DDB0184464	DDB0204659	DDB0190707
GENE	Pianissimo	LST8	TOR	3/3/14
# of peptides	72	5	27	2
total peptides	387	6	34	3
% ofcoverage	52.80%	23.00%	17.00%	18.90%
amino acids	1148	304	2380	244
M.W.	129529	33481	268748	27757

Locus	DDB0216574	DDB0190878	DDB0216574
GENE	hspD	HSP	HSP90
# of peptides	10	11	10
total peptides	22	18	22
% ofcoverage	25.30%	26.70%	25.30%
amino acids	700	64000.00%	700
M.W.	79866	70415	79866

Figure 4. TORC2 complex. (A and B) The coimmunoprecipitation of V5-tagged Pia with T7-tagged RIP3 (A) or T7-tagged LST8 (B). Cells were cotransformed with expression vectors expressing V5-Pia and T7-RIP3 or V5-Pia and T7-LST8 or expression on T7-RIP3 or only T7-LST8. The immunoprecipitation was carried out using anti-V5 antibody (see *Materials and Methods*) and the Western blot was probed (IB) with either anti-T7 or anti-V5 antibody as shown. TCL shows the protein in total cell lysates. (C) Partial list of peptides identified in the mass spectrometry analysis of the V5-Pia-containing complex. Proteins found in common with the control sample are not shown.

(GenBank accession no. DDB0191024), it is not present in these immunoprecipitates, suggesting that *Dictyostelium* forms a separate TORC1. Interestingly, we did not observe RIP3 in the complex, although it coimmunoprecipitates with Pia. These differences between the coimmunopreciptation data and the MS analysis could be due to instability of the complex and differential loss of some components during the purification and/or differences in the efficiency of peptide ionization in the MS, leading to different efficiencies of peptide recovery in the analysis, although this is unlikely given the dynamic range and sensitivity of the MS. Nevertheless, these findings indicate that, similar to the yeast and mammalian counterparts, *Dictyostelium* LST8, RIP3, and Pia form one or more TORC2 complexes (Loewith *et al.*, 2002; Jacinto *et al.*, 2004). We did not identify any orthologues to yeast AVO2 and no clear ortholog is found in the *Dictyostelium* genome database.

Dictyostelium TORC2 Regulates Cell Movement during Chemotaxis

An aggregation-deficient developmental phenotype can arise from defects in either ACA activation or chemotaxis, which are functionally independent (Comer et al., 2005). Previous studies suggested that *pia*$^-$ cells exhibit chemotaxis defects (Chen *et al.*, 1997) and demonstrated that *rip3*$^-$ cells have reduced cell polarity and a lower chemotaxis index (Lee *et al.*, 1999). To assess the ability of the *lst8*$^-$ cells to chemotax, we examined their chemotaxis toward a micropipette filled with cAMP. We quantified their behavior using DIAS computer software (Wessels *et al.*, 1988, 1998) and compared this strain to wild-type cells and *pia*$^-$ and *rip3*$^-$ cells, whose chemotaxis parameters had not been previously measured. We found that, although the *lst8*$^-$ cells can migrate toward the micropipette, they do so with reduced speed and directionality and with significant loss in polarity compared with wild-type cells (Figure 5, A and B; Table 1). *rip3*$^-$ cells showed similar defects, consistent with previous findings (Lee *et al.*, 1999). The chemotaxis defects of *pia*$^-$ cells were not as strong as those for *lst8*$^-$ and *rip3*$^-$ cells. To further characterize the chemotaxis defects of *rip3*$^-$, *pia*$^-$, and *lst8*$^-$ cells, we analyzed the mutants using the under-agarose assay (Laevsky and Knecht, 2001; Comer *et al.*, 2005), in which cells migrate under a layer of agarose in a gradient of chemoattractant. Under these conditions, the *lst8*$^-$ cells, as well as the *rip3*$^-$ and *pia*$^-$ cells, do not migrate as far toward the cAMP source as wild-type cells and, most notably, do not organize into streams, a process that requires ACA activation (Kriebel *et al.*, 2003; unpublished data). These data are consistent with the notion that LST8, RIP3, and Pia function together in a complex that regulates both ACA activation/signal relay and chemotaxis.

Proper chemotaxis requires the concerted regulation of anterior F-actin extension and posterior myosin II contraction (Ridley *et al.*, 2003). We therefore examined whether deficiencies in LST8, RIP3, or Pia result in defective chemoattractant-mediated F-actin polymerization or myosin II assembly. The *lst8*$^-$ cells exhibit a nominal but reproducible reduction in the extent of chemoattractant-stimulated F-actin polymerization in both the first (~5-s) and second (~45-s) peaks of activation, which correlate with the initial cringe response and the subsequent pseudopod extension, respectively, observed after uniform chemoattractant stimulation (Hall *et al.*, 1988; Figure 5C). The *rip3*$^-$ and *pia*$^-$ cells experience a similar modest decrease in the first peak, but the level of the second F-actin peak is indistinguishable from that of wild-type cells. We do not think that any change in

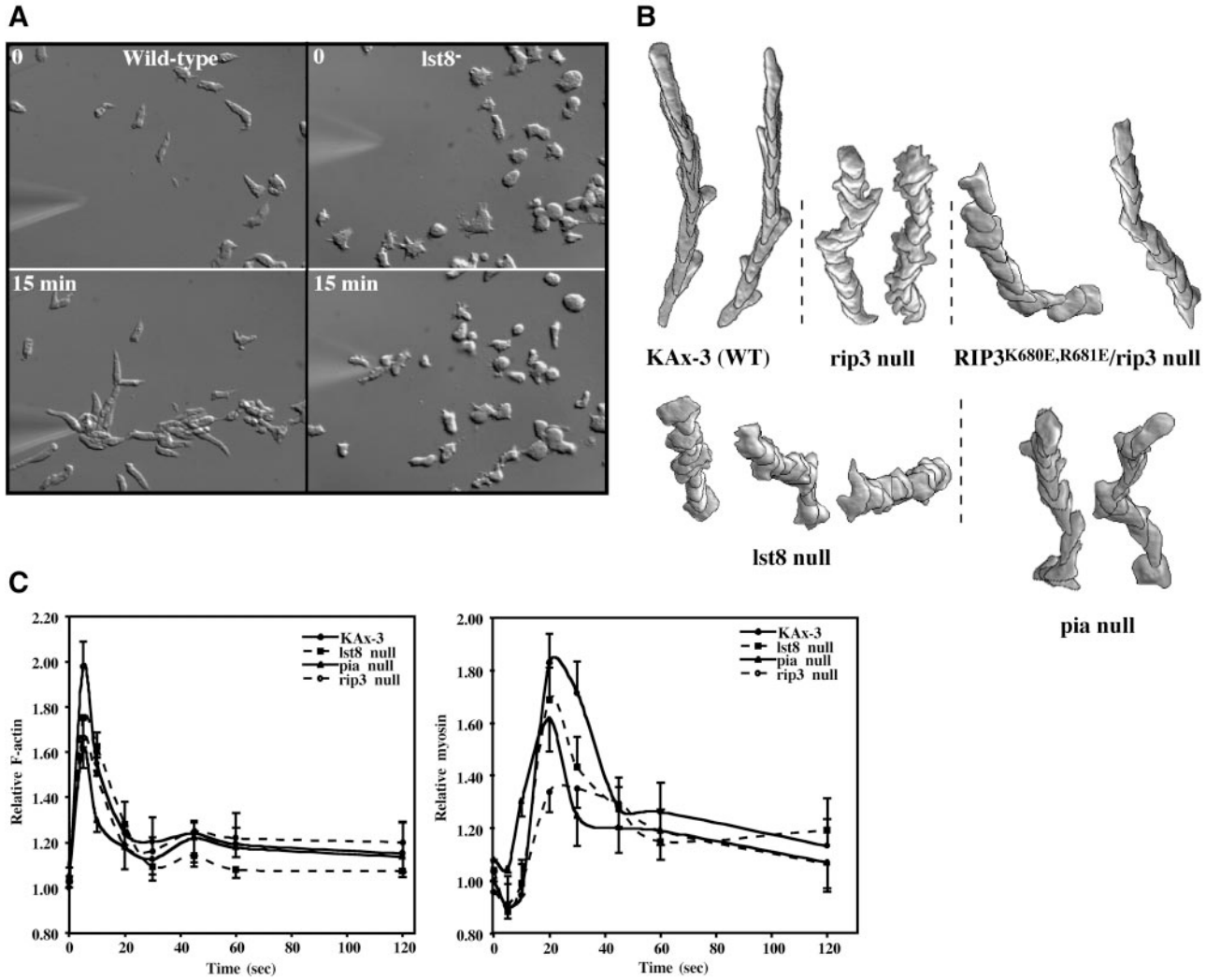

Figure 5. Chemotaxis properties of TORC2 mutant strains. (A) Chemotaxis images of wild-type (KAx-3) and *lst8*$^{-}$ cells using DIC optics. Images shown are taken at the time the micropipette containing the chemoattractant is inserted (0 time) and at 15 min. See *Materials and Methods* for details. (B) Images of chemotaxing cells obtained using DIAS computer software (see *Materials and Methods*). The overlapping images are taken at 1-min intervals. (C) Chemoattractant stimulated F-actin polymerization and myosin II assembly as described in the *Materials and Methods*.

the first F-actin peak that is observed is at all responsible for the null polarity and chemotaxis defects. All three mutant strains exhibit moderately altered patterns of chemoattractant-mediated myosin II assembly. In wild-type cells, the levels of myosin II associated with the cytoskeleton undergo an initial slight decrease 5–10 s after uniform chemoattrac-

Table 1. DIAS analysis

					RIP3		
					K680E,R681E		
Strain	KAx-3	*lst*8 null	pia null	*rip*3 null	KAx-3	*rip*3 null	*rip*3 null
Speed (um/min)	9.96 ± 0.70	5.39 ± 0.38	7.41 ± 0.25	5.36 ± 1.97	10.2 ± 2.12	9.37 ± 0.18	6.70 ± 0.82
Dir ch (deg)	24.1 ± 4.06	40.4 ± 6.62	41.1 ± 0.56	46.8 ± 9.84	16.0 ± 3.10	30.9 ± 5.64	32.2 ± 4.09
Roundness	52.4 ± 3.04	75.8 ± 3.46	66.3 ± 1.29	62.2 ± 3.62	54.3 ± 3.93	60.5 ± 5.78	71.0 ± 2.48
Directionality	0.78 ± 0.01	0.57 ± 0.10	0.48 ± 0.01	0.53 ± 0.12	0.84 ± 0.02	0.74 ± 0.04	0.57 ± 0.04

DIAS analysis of chemotaxis. Numbers are mean values ± SD. Speed indicates speed of cell's centroid movement along the total path. Direction change is a relative measure of the number and frequency of turns the cell makes. Larger numbers indicate more turns and less efficient chemotaxis. Directionality is a measure of the linearity of the pathway. Cells moving in a straight line to the needle have a directionality of 1.00. Roundness is an indication of the polarity of the cells. Larger numbers indicate the cells are more round (less polarized).

A

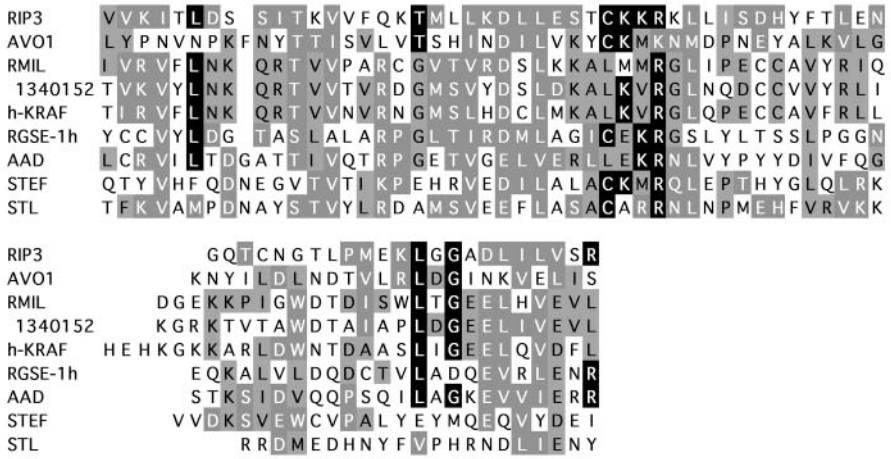

B

RIP3 mutant	Yeast 2-hybrid Bait RasG Q61L	Ability to aggregate Overexpressed in *rip3*null
Wild-type	+++++	+++++
K680E R681E	-	+

C

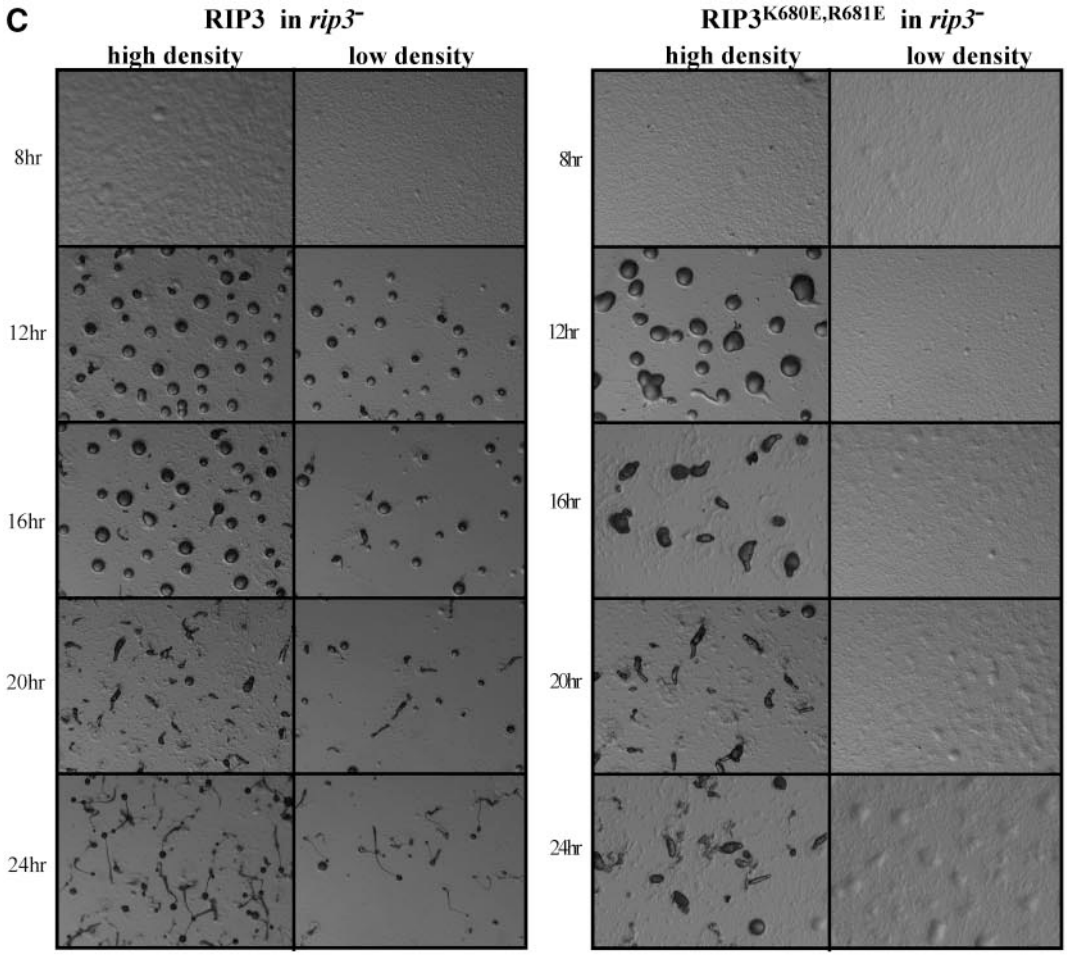

Figure 6.

tant stimulation and then increase about twofold, peaking at ~30 s, before decreasing to basal levels (Steimle *et al.,* 2001; Park *et al.,* 2004). The *rip3*$^-$ cells exhibit the strongest phenotype, with a significantly reduced peak of myosin II assembly upon chemoattractant stimulation (Figure 5C). The essentially wild-type F-actin response and moderate defects in myosin II assembly suggest that these cells do not have a fundamental inability to undergo cytoskeletal changes in response to chemoattractant. However, all three null strains simultaneously extend random pseudopodia from multiple points around the entire periphery of the cell, in contrast to wild-type cells, which predominantly extend pseudopodia in the direction of the chemoattractant gradient. The poor directionality of chemotaxing of the *rip3*$^-$, *pia*$^-$, and *lst8*$^-$ cells supports the hypothesis that at least part of the loss of directionality results from more random movement inherent in cells that form multiple lateral pseudopodia. Our data, however, do not exclude the possibility that these cells show a defect in gradient interpretation or spatial-temporal signaling to the cytoskeleton. This possibility is strongest for *lst8*$^-$ cells as some of these cells exhibit directionality defects that are stronger than those exhibited by the other strains and for other apolar mutants such as *myoII*$^-$ or *pakB/pakC*$^{-/-}$ cells (Wessels *et al.,* 1988; Lee *et al.,* 2004).

Ras Is Involved in the Regulation of RIP3

RIP3 was identified in a yeast two-hybrid screen using constitutively active human H-Ras as bait and was found to interact with GTP-bound forms of *Dictyostelium* RasG and human H-Ras (Lee *et al.,* 1999). Sequence comparison identified a putative Ras-binding domain (RBD) in RIP3 (Figure 6A). The Arg residue at position 681 is conserved in many of these domains, suggesting it might be important for mediating interactions between the RBD and Ras-GTP. We examined this by mutating this Arg and the preceding Lys to Glu (K680E, R681E) and found that the RIP3 RBD carrying these substitutions no longer interacted with RasG-GTP in a two-hybrid assay (Figure 6B). Expression of wild-type RIP3 complemented the developmental and chemotaxis defects of *rip3*$^-$ cells (Figure 6C; Table 1). The chemotaxis parameters were slightly reduced compared with wild-type cells, but they were similar to wild-type cells overexpressing RIP3, suggesting any changes were due to an overexpression of RIP3 protein (Table 1; Figure 5A). In contrast, when RIP3^{K680E,R681E} was expressed in *rip3*$^-$ cells, it only partially complemented the developmental and chemotaxis defects. *rip3*$^-$ cells expressing RIP3^{K680E,R681E} form aggregates at higher cell densities where cell-cell contacts can assist in aggregate formation but the organisms exhibit developmental defects and are delayed in morphogenesis. The cells cannot aggregate at lower cell densities where chemotaxis plays an increasingly important role. Similar effects have been noted for several signaling mutants, including *akt/pkb* null cells (Meili *et al.,* 1999). Further, *rip3*$^-$ cells expressing RIP3^{K680E,R681E} exhibit only a small improvement in chemotaxis speed, and the directionality of movement, an indicator of chemotaxis index, is similar to that of *rip3*$^-$ cells. These results suggest that a functional RBD is important for full RIP3 function.

Figure 6 (facing page). Analysis of RIP3. (A) Sequence comparison of RIP3 Ras-binding domain. RIP3 (AAD43567, *D. discoideum*); AVO1 (NP_014563, *S. cerevisiae*); RMIL/v-Raf1 (EAL24023, *Homo sapiens*); 1340152/A-Raf1 (AAH07514, *H. sapiens*), h-KRAF (AAP03432, *H. sapiens*); RGSE-1h/RGS14 (043566, *H. sapiens*); AAD/CG5248-PL (NP_732776, *Drosophila melanogaster*); STEF (NP_036008, *Mus musculus*); STL (NP_524647, *D. melanogaster*). (B) Two-hybrid interaction of wild-type RIP3 and RIP3^{K680E,R681E} with constitutively active *Dictyostelium* RasG (RasG^{Q61L}). (C) Development of *rip3*$^-$ cells expressing RIP3 or RIP3^{K680E,R681E} plated on nonnutrient agar at high ($3 \times 10^6/cm^2$) and low ($0.75 \times 10^6/cm^2$) density.

Dictyostelium TORC2 Acts Downstream of Ras and PI3K

Numerous studies have shown that PI3 kinases (PI3Ks) play multiple roles in chemoattractant signaling in *Dictyostelium* and mammalian leukocytes (Funamoto *et al.,* 2001; Stephens *et al.,* 2002; Merlot and Firtel, 2003; Van Haastert and Devreotes, 2004). Cells lacking PI3K function exhibit chemotaxis defects similar to those of the *rip3*$^-$, *pia*$^-$, and *lst8*$^-$ cells (Funamoto *et al.,* 2001, 2002; Sasaki *et al.,* 2004). In *Dictyostelium*, PI3K1 and PI3K2 translocate from the cytosol to the leading edge membrane during chemotaxis and removal of the membrane-targeting domain impairs chemoattractant signaling through PI3K (Funamoto *et al.,* 2002). Ras-mediated activation of PI3K is thought to preferentially promote localized activation of the chemotactic machinery, thus sharply amplifying chemoattractant signaling at the leading edge of chemotaxing cells (Sasaki *et al.,* 2004). To gain insight into the mechanism by which TORC2 regulates chemotaxis and signal relay, we studied the impact of TORC2 on PI3K signaling pathways. We first assessed the extent of chemoattractant-stimulated Ras activation in the TORC2 mutants using a pulldown assay in which GTP-bound Ras is isolated through its binding to the RBD of human Raf1 and then quantified using a Western blot assay (Sasaki *et al.,* 2004). This assay examines the activation of RasG, RasD, and RasB with the majority of the Ras-GTP bound to the Raf1-RBD in aggregation-competent cells attributed to RasG (Sasaki *et al.,* 2004). As depicted in Figure 7A, all strains exhibited kinetics and extent of Ras activation similar to those of wild-type cells. We next assessed the role of the TORC2 components RIP3, Pia, and LST8 in the cellular distribution of PI3K. We transformed wild-type, *rip3*$^-$, *pia*$^-$, and *lst8*$^-$ cells with GFP-N-PI3K1, which is necessary and sufficient for PI3K1 cortical localization, and studied its distribution in chemotaxing cells. As previously reported, we observed that the majority of the cortically localized GFP-N-PI3K1 is found at the leading edge of wild-type chemotaxing cells. Because of improved imaging technology, we now also find that a smaller fraction of GFP-N-PI3K1 localizes at the cell posterior (Figure 8). Both localizations are sites of enriched F-actin polymerization, consistent with our demonstration that enhanced GFP-N-PI3K cortical localization is dependent on new F-actin (Sasaki *et al.,* 2004). As expected, wild-type cells have a ruffled leading edge with numerous protrusions. In contrast, *rip3*$^-$, *pia*$^-$, and *lst8*$^-$ cells have broader GFP-N-PI3K1-containing domains with multiple lateral pseudopodia and broader posteriors, illustrating their loss-of-polarity phenotype (Figures 5, A and B, and 8; data for *pia*$^-$ cells are not published). Nevertheless, we find that GFP-N-PI3K1 is targeted to the cortex in the mutants. Furthermore, we observed that the mutant cell lines have normal kinetics of GFP-N-PI3K1 translocation to the cortex in response to uniform chemoattractant stimulation (unpublished data). These data demonstrate that the TORC2 components are not required for Ras activation or for the spatial targeting of PI3K.

We next evaluated whether the components of TORC2 regulate PI3K activation, using translocation of the CRAC and PhdA PH domain to the plasma membrane as markers for the accumulation of PI(3,4,5)P_3, the major product of PI3K. Earlier studies demonstrated that chemoattractant-mediated translocation of CRAC and PhdA to the plasma membrane is a G protein-, PI3K-, and PH domain-dependent

event (Parent *et al.*, 1998; Funamoto *et al.*, 2001, 2002). Figure 7, B–D, depict the plasma membrane translocation of PH_{CRAC}-GFP in *rip3*$^-$, *pia*$^-$, and *lst8*$^-$ cells following a uniform, saturating dose of chemoattractant, as judged by both fluorescence microscopy and Western blot analysis of membrane preparations (data for PhdA not published). All three mutant cell lines retain the capacity to generate membrane binding sites for PH_{CRAC}-GFP and PhdA, displaying normal kinetics and an extent of translocation similar to that of wild-type cells. From these data, we infer that RIP3, Pia, and LST8 are not directly required to activate PI3K.

To gain further insight into the impact of TORC2 on PI3K signaling pathways, we examined activation of the PI3K-regulated effector PKB in *rip3*$^-$, *pia*$^-$, and *lst8*$^-$ cells by directly measuring the chemoattractant-mediated activation of PKB. Surprisingly, we found that in *rip3*$^-$ and *pia*$^-$ cells exhibit a significant impairment in PKB activation compared with wild-type cells (Figure 7D). PKB activation was less impaired in *lst8*$^-$ cells, although the activation was still reproducibly lower than that of wild-type cells (Figure 7D). Combined with our observation that CRAC and PhdA translocation/PI3K activation is not impaired in the TORC2 mutants, these data are consistent with a model in which TORC2 acts either downstream or parallel to PI3K in the chemoattractant-mediated activation of PKB.

Dictyostelium cells express two distinct PKB-related kinases, PKB (the ortholog of mammalian PKB) and PKBR1. PKBR1 is required for morphogenesis during the multicellular stages of *Dictyostelium* development (Meili *et al.*, 2000). It harbors highly conserved kinase and C-terminal hydrophobic domains that include conserved sites of phosphorylation equivalent to T^{308} and S^{473} in human PKB. However, in contrast to PKB, PKBR1 lacks a true PH domain (it has an N-terminal, PH-like domain) and localizes constitutively to the plasma membrane via an N-terminal myristoylation modification. PKBR1 is activated by chemoattractants in a PI3K-independent manner, presumably because PKBR1 is constitutively associated with the plasma membrane and does not require de novo PtdIns(3,4,5)P_3 synthesis for its membrane localization. *pkbr1*$^-$ cells exhibit very weak chemotaxis phenotypes but a double PKB/PKBR1 null strain has strong growth and chemotaxis defects, indicating that both kinases control chemotaxis pathways. These phenotypes are more severe than those of *rip3*$^-$, *pia*$^-$, and *lst8*$^-$ cells and significantly more severe than those of *pkb*$^-$ cells. We therefore examined the extent of chemoattractant-induced PKBR1 phosphorylation in *rip3*$^-$, *pia*$^-$, and *lst8*$^-$ cells. Remarkably, as with PKB, PKBR1 phosphorylation is impaired in *rip3*$^-$ and *pia*$^-$ cells and less affected in *lst8*$^-$ cells (Figure 6E), further indicating that the defect in PKB phosphorylation is not a result of improper targeting to the plasma membrane or defects in PI3K activation. Rather, these results are consistent with the *Dictyostelium* TORC2 regulating the phosphorylation of PKB and PKBR1. Although the effects on cell movement are strongest in *lst8*$^-$ cells, these cells exhibit the weakest effect on PKB and PKBR1 activation. These observations suggest that different components of the TORC2 complex have different effects on TOR activity in different pathway. Our data do not exclude the possibility of multiple TORC2 complexes with different or overlapping functions or activities.

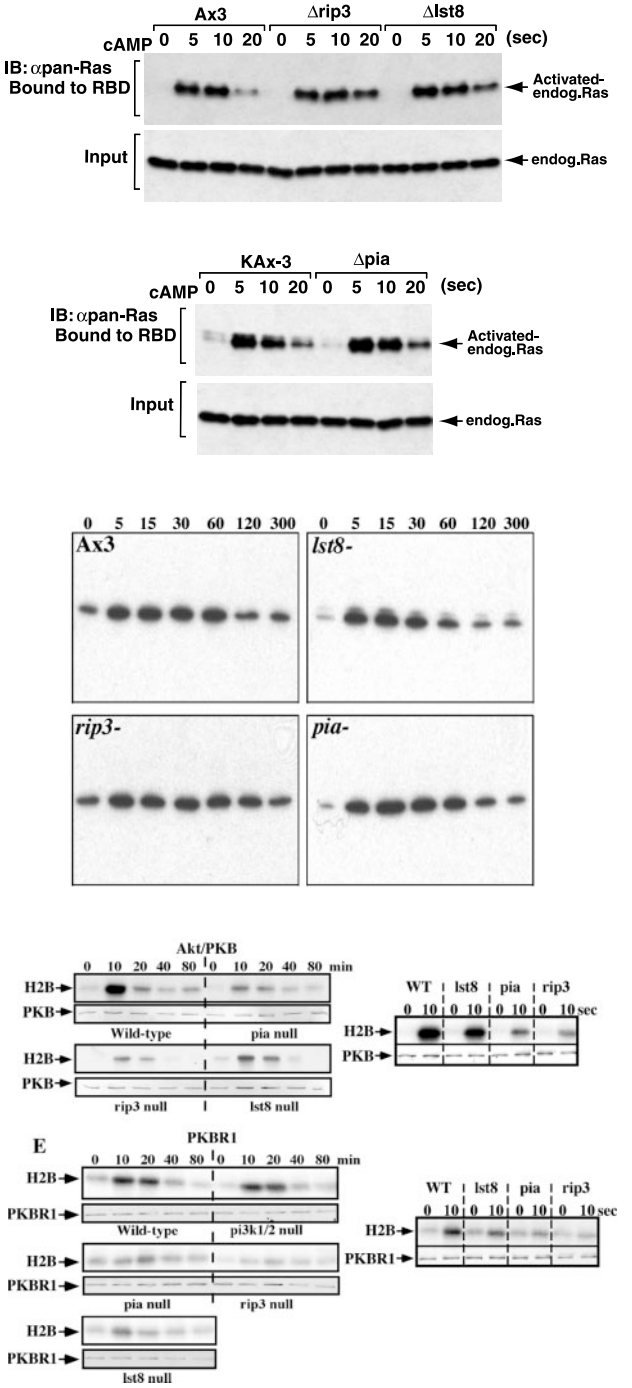

Figure 7. Regulation of the PI3K pathway in TORC2 mutants. (A) Ras activation in wild-type and *lst8*$^-$, *rip3*$^-$, and *pia*$^-$ cells is shown. (B and C) Translocation of PH_{CRAC}-GFP to the cortex examined biochemically (B) or by fluorescence microscopy (C). (D and E) Chemoattactant-mediated activation (kinase assay) of Akt/PKB (D) and PKBR1 (E) in wild-type and *lst8*$^-$, *rip3*$^-$, and *pia*$^-$ cells. Activation of PKBR1 in *pi3k1/2* null cells is also shown (E). Histone 2B (H2B) is used as a substrate. Upper lanes show the kinase assay. Lower lanes show a Western blot of Akt/PKB or PKBR1 protein in the immunoprecipitate. See *Materials and Methods* for details.

DISCUSSION

The Composition of Dictyostelium TORC2

We demonstrate here that *Dictyostelium* cells express a TORC2 that is essential for multicellular development, but not growth. As in *S. cerevisiae*, *Dictyostelium* Pia, RIP3, and LST8, the orthologues of yeast AVO3, AVO1, and LST8, form a complex in vivo. Our MS analyses of Pia-containing

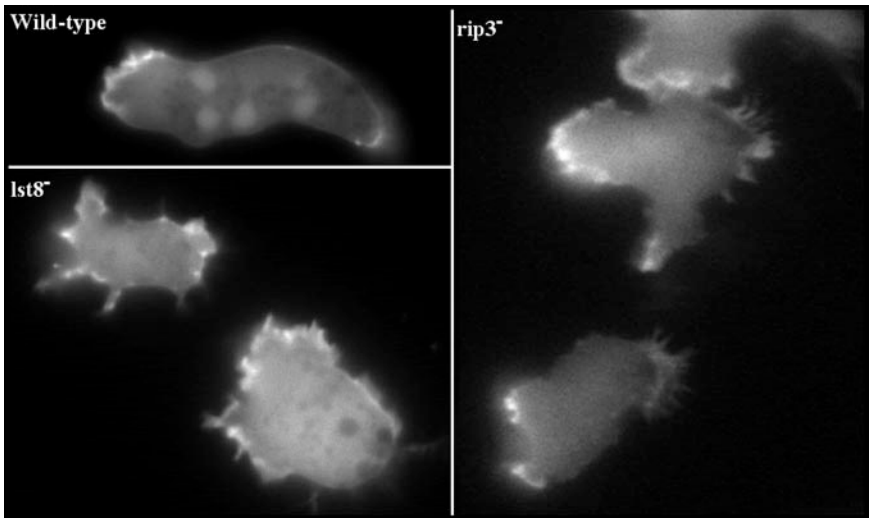

Figure 8. PI3K localization in chemotaxing cells. Fluorescent images of GFP-N-PI3K1, a reporter for the localization of PI3K, are taken from real-time digital recordings of *lst8*$^-$, *rip3*$^-$, and wild-type chemotaxing cells (Funamoto *et al.,* 2001; Sasaki *et al.,* 2004). The micropipette is located to the left of the cells off the field of view.

complexes identified TOR and LST8 but not Raptor, which is present in the *Dictyostelium* genome and is a known component of rapamycin-sensitive TORC1 in other systems (Lorberg and Hall, 2004). Although RIP3 was not observed in the MS analysis of Pia-containing complexes, coimmunoprecipitation experiments determined it is associated with Pia in vivo. Although rapamycin inhibits growth in *Dictyostelium*, presumably through TORC1, our studies indicate that TORC2 is rapamycin-insensitive, because the signaling pathways that are genetically controlled by TORC2 are not inhibited by the drug. This is consistent with the findings in yeast and mammalian cells, although we have not formally proven the existence of an independent TORC1 biochemically (Loewith *et al.,* 2002; Jacinto *et al.,* 2004; Sarbassov dos *et al.,* 2004). As cells lacking Pia, RIP3, or LST8 do not have growth defects, it is clear that a rapamycin-sensitive TOR complex that does not contain Pia, RIP3, or LST8 controls growth in *Dictyostelium* (Lorberg and Hall, 2004). Furthermore, our attempts to create a cell line lacking the single TOR gene found in the *Dictyostelium* genome (http://dictybase.org) were unsuccessful, consistent with our rapamycin results and showing that TOR is required for growth.

Our attempts to purify *Dictyostelium* TORC2 suggest that the complex is not very stable, and we obtained the best coimmunoprecipitation results using chemical cross-linking. Our biochemical findings, combined with the common phenotypes of *rip3*$^-$, *pia*$^-$, and *lst8*$^-$ cells, provide strong indications of a *Dictyostelium* TORC2 that minimally contains TOR, LST8, RIP3, and Pia. Intriguingly, our MS analyses revealed that 14-3-3 and several heat-shock proteins are associated with Pia, the latter of which we assume function as molecular chaperones, possibly to help form or stabilize TORC2. 14-3-3 may further stabilize the complex or TOR by bridging phosphoserine residues.

TORC2 Integrates Signaling Pathways Regulating Aggregation

Previous studies and those presented here show that *rip3*$^-$, *pia*$^-$, and *lst8*$^-$ null strains all share common phenotypes: the inability to activate adenylyl cyclase in response to chemoattractant signaling; and a severe loss of cell polarization, directionality in movement, and chemotaxis speed (Chen *et al.,* 1997; Lee *et al.,* 1999). Using reconstitution of these null cell lines, we provide strong evidence that Pia, RIP3, and LST8 function together in a preformed complex to regulate ACA. The mechanism by which this occurs remains to be determined. Our reconstitution experiments demonstrate that TORC2 is formed in the absence of CRAC, a PI3K effector required for the activation of adenylyl cyclase. It was previously established that ACA activity can be reconstituted in lysates derived from cells lacking both Pia and CRAC only when both proteins are added back (Chen *et al.,* 1997), suggesting that ACA activation requires an input from both TORC2 and CRAC.

We also demonstrate that *rip3*$^-$, *pia*$^-$, and *lst8*$^-$ cells exhibit a reduction in chemoattractant-mediated activation of Akt/PKB and PKBR1, a PKB-related kinase that is also activated by phosphorylation of a conserved site in the activation loop and C-terminal hydrophobic residues corresponding to T308 and S473, respectively, in human PKB (Alessi *et al.,* 1996, 1997; Williams *et al.,* 2000). It was recently shown that TORC2 directly phosphorylates PKB on S473 in *Drosophila* Kc_{167} cells as well as in a variety of human cell lines (Sarbassov *et al.,* 2005). Our data strongly suggest that TORC2 acts in a similar manner in *Dictyostelium*, in which the reduced chemoattractant-mediated phosphorylation of PKB and PKBR1 could due to the specific loss of phosphorylation in the C-terminal domain. Consistent with this model, we find that although Akt/PKB activation in *Dictyostelium* is PI3K-dependent (Meili *et al.,* 1999), as it is in mammalian cells, the PI3K pathway and the activation of Ras, which lies upstream of PI3K, is not detectably affected in *lst8*$^-$, *pia*$^-$, and *rip3*$^-$ cells. A complete loss of both Akt/PKB and PKBR1 in *Dictyostelium* results in chemotaxis phenotypes significantly more severe than those of *rip3*$^-$, *pia*$^-$, and *lst8*$^-$ cells (Meili *et al.,* 1999, 2000). It is currently difficult to determine if the observed partial loss of PKB and PKBR1 phosphorylation is responsible for the chemotaxis and polarity defects of the *rip3*$^-$, *pia*$^-$, and *lst8*$^-$ cells, as we expect the TORC2 pathway to control other chemoattractant signals. Furthermore, we do not know whether TORC2 activity is constitutive or stimulated in response to chemoattractant. Although we expect the latter, presently we have no way of directly assaying this.

A commonality of the yeast, mammalian cell, and *Dictyostelium* TORC2 pathways is a loss of cell polarity (Schmidt *et al.,* 1996; Chen *et al.,* 1997; Lee *et al.,* 1999; Jacinto *et al.,* 2004; Sarbassov dos *et al.,* 2004). *Dictyostelium* TORC2 mutants produce multiple pseudopodia simultaneously along the

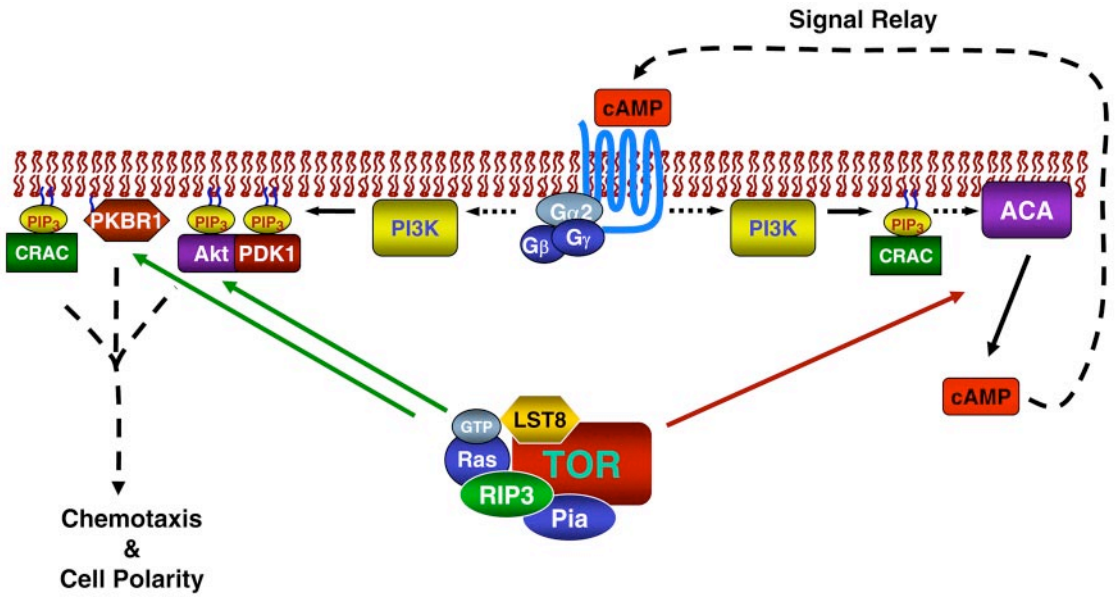

Figure 9. Model of TORC2 function during chemotaxis. Receptor activation of signal relay and chemotaxis focusing on the PI3K pathway is shown. Cyclical AMP activation of the cAMP receptor cAR1 activates the G protein containing Gα2 and G$\beta\gamma$. Activation of Ras through a Ras GEF (unpublished data) leads to activation of PI3K and the production of PI(3,4,5)P_3 and the translocation of PH domain-containing proteins. These include Akt/PKB, PhdA and CRAC (PhdA; unpublished data). PKBR1 is constitutively localized to the plasma membrane. PTEN is a negative regulator. Akt/PKB and PKBR1 are activated via PDK1 and TORC2. Receptor activation of adenylyl cyclase A (ACA) requires the same receptor/heterotrimeric G protein complex and CRAC. The cAMP produced activates PKA intracellularly and is secreted into the medium to activate receptors on neighboring cells.

cell's cortex when placed in a chemoattractant gradient. We find that *lst8*$^-$, *rip3*$^-$, and *pia*$^-$ cells have reduced chemoattractant-mediated F-actin polymerization and myosin II assembly, with the strongest defect in myosin II assembly observed in *rip3*$^-$ cells. The reduced myosin II assembly may be due to the reduction in Akt/PKB activity, which is required for maximal myosin II assembly in *Dictyostelium* (Chung *et al.*, 2001). In yeast and mammalian cells, TORC2 functions, at least in part, by controlling protein kinase C and/or Rho GEF activity, although a direct link between these signaling pathways, TORC2, and polarity has yet to be established (Schmidt *et al.*, 1997; Jacinto and Hall, 2003; Jacinto *et al.*, 2004; Lorberg and Hall, 2004). In *Dictyostelium*, loss of cell polarity during chemotaxis is at least partially due to reduced Akt/PKB and PKBR1 activation.

Aggregation to form a multicellular organism in *Dictyostelium* requires the integration of signal relay (the activation and secretion of the chemoattractant cAMP) with chemotaxis (Aubry and Firtel, 1999; Kimmel and Parent, 2003). We have shown that TORC2 is required for chemotaxis, cell polarity, and activation of ACA. TORC2 therefore coordinates the activation of distinct signaling pathways required for a common biological response (see model in Figure 9). We propose that, in vivo, TORC2 provides a rapidly mobilizable module that can respond quickly to extracellular chemoattractant signals, thus providing an efficient way to modulate complex responses. Interestingly, ACA and PKB activation requires input from PI3K and TORC2, which are both regulated by Ras-GTP (Funamoto *et al.*, 2002; Sasaki *et al.*, 2004). We previously discovered that the RIP3 RBD binds RasG-GTP, which is required for proper cell polarity and chemotaxis (Tuxworth *et al.*, 1997; Lee *et al.*, 1999; Funamoto *et al.*, 2002; Sasaki *et al.*, 2004). We now demonstrate that RIP3 carrying a point mutation that abrogates RasG-GTP binding cannot fully complement the *rip3*$^-$ mutation, suggesting that Ras-GTP/RIP3 interaction is required for full RIP3/TORC2 function. A recent study indicates that strains in which Ras function is severely abrogated display a loss of directionality and ability to directionally respond to the chemoattractant gradient during chemotaxis (Sasaki *et al.*, 2004). The fact that this phenotype is significantly stronger than those of cells lacking PI3K1 and PI3K2 is consistent with Ras playing other parts during chemotaxis. We propose that TORC2 is one of these Ras-regulated processes. This complex level of coordinated control of chemotaxis and signal relay is consistent with other complex feedback loops that regulate leading edge formation in both neutrophils and *Dictyostelium* cells (Weiner *et al.*, 2002; Park *et al.*, 2004; Sasaki *et al.*, 2004). Regulatory controls, such as those imposed by TORC2, thus provide cells with additional layers of flexibility for the coordination of complex physiological responses such as *Dictyostelium* aggregation.

ACKNOWLEDGMENTS

F.I.C. is a recipient of the National Institute of General Medical Sciences Pharmacology Research Associate Training Fellowship. This work was supported in part by US Public Health Service Grants RR11823-09 to J.R.Y. and GM37830 to R.A.F.

REFERENCES

Alessi, D. R., Andjelkovic, M., Caudwell, B., Cron, P., Morrice, N., Cohen, P., and Hemmings, B. A. (1996). Mechanism of activation of protein kinase B by insulin and IGF-1. EMBO J. *15*, 6541–6551.

Alessi, D. R., James, S. R., Downes, C. P., Holmes, A. B., Gaffney, P. R., Reese, C. B., and Cohen, P. (1997). Characterization of a 3-phosphoinositide-dependent protein kinase which phosphorylates and activates protein kinase Balpha. Curr. Biol. *7*, 261–269.

Aubry, L., and Firtel, R. (1999). Integration of signaling networks that regulate *Dictyostelium* differentiation. Annu. Rev. Cell Dev. Biol. *15*, 469–517.

Chen, M. Y., Long, Y., and Devreotes, P. N. (1997). A novel cytosolic regulator, pianissimo, is required for chemoattractant receptor and G protein-mediated activation of the 12 transmembrane domain adenylyl cyclase in *Dictyostelium.* Genes Dev. *11*, 3218–3231.

Chung, C. Y., Potikyan, G., and Firtel, R. A. (2001). Control of cell polarity and chemotaxis by Akt/PKB and PI3 kinase through the regulation of PAKa. Mol. Cell *7*, 937–947.

Comer, F. I., Lippincott, C. K., Masbad, J. J., and Parent, C. A. (2005). The PI3K-mediated activation of CRAC independently regulates adenylyl cyclase activation and chemotaxis. Curr. Biol. *15*, 134–139.

Funamoto, S., Meili, R., Lee, S., Parry, L., and Firtel, R. A. (2002). Spatial and temporal regulation of 3-phosphoinositides by PI 3-kinase and PTEN mediates chemotaxis. Cell *109*, 611–623.

Funamoto, S., Milan, K., Meili, R., and Firtel, R. A. (2001). Role of phosphatidylinositol 3′ kinase and a downstream pleckstrin homology domain-containing protein in controlling chemotaxis in *Dictyostelium.* J. Cell Biol. *153*, 795–809.

Hall, A. L., Schlein, A., and Condeelis, J. (1988). Relationship of pseudopod extension to chemotactic hormone-induced actin polymerization in amoeboid cells. J. Cell. Biochem. *37*, 285–299.

Hay, N., and Sonenberg, N. (2004). Upstream and downstream of mTOR. Genes Dev. *18*, 1926–1945.

Insall, R., Kuspa, A., Lilly, P. J., Shaulsky, G., Levin, L. R., Loomis, W. F., and Devreotes, P. (1994). CRAC, a cytosolic protein containing a pleckstrin homology domain, is required for receptor and G protein-mediated activation of adenylyl cyclase in *Dictyostelium.* J. Cell Biol. *126*, 1537–1545.

Insall, R. H., Borleis, J., and Devreotes, P. N. (1996). The aimless RasGEF is required for processing of chemotactic signals through G-protein-coupled receptors in *Dictyostelium.* Curr. Biol. *6*, 719–729.

Jacinto, E., and Hall, M. N. (2003). Tor signalling in bugs, brain and brawn. Nat. Rev. Mol. Cell. Biol. *4*, 117–126.

Jacinto, E., Loewith, R., Schmidt, A., Lin, S., Ruegg, M. A., Hall, A., and Hall, M. N. (2004). Mammalian TOR complex 2 controls the actin cytoskeleton and is rapamycin insensitive. Nat. Cell Biol. *6*, 1122–1128.

Kimmel, A. R., and Parent, C. A. (2003). *Dictyostelium discoideum* cAMP chemotaxis pathway. In: http://stke.sciencemag.org/cgi/cm/CMP_7918.

Kriebel, P. W., Barr, V. A., and Parent, C. A. (2003). Adenylyl cyclase localization regulates streaming during chemotaxis. Cell *112*, 549–560.

Laevsky, G., and Knecht, D. A. (2001). Under-agarose folate chemotaxis of *Dictyostelium discoideum* amoebae in permissive and mechanically inhibited conditions. Biotechniques *31,* 1140–1149.

Lee, S., Parent, C. A., Insall, R., and Firtel, R. A. (1999). A novel Ras-interacting protein required for chemotaxis and cyclic adenosine monophosphate signal relay in *Dictyostelium.* Mol. Biol. Cell *10*, 2829–2845.

Lee, S., Rivero, F., Park, K. C., Huang, E., Funamoto, S., and Firtel, R. A. (2004). *Dictyostelium* PAKc is required for proper chemotaxis. Mol. Biol. Cell *15*, 5456–5469.

Lilly, P. J., and Devreotes, P. N. (1995). Chemoattractant and GTP gamma S-mediated stimulation of adenylyl cyclase in *Dictyostelium* requires translocation of CRAC to membranes. J. Cell Biol. *129*, 1659–1665.

Loewith, R., Jacinto, E., Wullschleger, S., Lorberg, A., Crespo, J. L., Bonenfant, D., Oppliger, W., Jenoe, P., and Hall, M. N. (2002). Two TOR complexes, only one of which is rapamycin sensitive, have distinct roles in cell growth control. Mol. Cell *10*, 457–468.

Lorberg, A., and Hall, M. N. (2004). TOR: the first 10 years. Curr. Top. Microbiol. Immunol. *279*, 1–18.

Meili, R., Ellsworth, C., and Firtel, R. A. (2000). A novel Akt/PKB-related kinase is essential for morphogenesis in *Dictyostelium.* Curr. Biol. *10*, 708–717.

Meili, R., Ellsworth, C., Lee, S., Reddy, T., Ma, H., and Firtel, R. (1999). Chemoattractant-mediated transient activation and membrane localization of Akt/PKB is required for efficient chemotaxis to cAMP in *Dictyostelium.* EMBO J. *18*, 2092–2105.

Merlot, S., and Firtel, R. A. (2003). Leading the way: directional sensing through phosphatidylinositol 3-kinase and other signaling pathways. J. Cell Sci. *116*, 3471–3478.

Parent, C., Blacklock, B., Froehlich, W., Murphy, D., and Devreotes, P. (1998). G protein signaling events are activated at the leading edge of chemotactic cells. Cell *95*, 81–91.

Parent, C. A., and Devreotes, P. N. (1995). Isolation of inactive and G protein-resistant adenylyl cyclase mutants using random mutagenesis. J. Biol. Chem. *270*, 22693–22696.

Parent, C. A., and Devreotes, P. N. (1996). Molecular genetics of signal transduction in *Dictyostelium.* Annu. Rev. Biochem. *65*, 411–440.

Park, K. C., Rivero, F., Meili, R., Lee, S., Apone, F., and Firtel, R. A. (2004). Rac regulation of chemotaxis and morphogenesis in *Dictyostelium.* EMBO J. *23*, 4177–4189.

Ridley, A. J., Schwartz, M. A., Burridge, K., Firtel, R. A., Ginsberg, M. H., Borisy, G., Parsons, J. T., and Horwitz, A. R. (2003). Cell migration: integrating signals from front to back. Science *302*, 1704–1709.

Sarbassov, D. D., Guertin, D. A., Ali, S. M., and Sabatini, D. M. (2005). Phosphorylation and regulation of Akt/PKB by the rictor-mTOR complex. Science *307*, 1098–1101.

Sarbassov dos, D., Ali, S. M., Kim, D. H., Guertin, D. A., Latek, R. R., Erdjument-Bromage, H., Tempst, P., and Sabatini, D. M. (2004). Rictor, a novel binding partner of mTOR, defines a rapamycin-insensitive and raptor-independent pathway that regulates the cytoskeleton. Curr. Biol. *14*, 1296–1302.

Sasaki, A. T., Chun, C., Takeda, K., and Firtel, R. A. (2004). Localized Ras signaling at the leading edge regulates PI3K, cell polarity, and directional cell movement. J. Cell Biol. *167*, 505–518.

Schmidt, A., Bickle, M., Beck, T., and Hall, M. N. (1997). The yeast phosphatidylinositol kinase homolog TOR2 activates RHO1 and RHO2 via the exchange factor ROM2. Cell *88*, 531–542.

Schmidt, A., Kunz, J., and Hall, M. N. (1996). TOR2 is required for organization of the actin cytoskeleton in yeast. Proc. Natl. Acad. Sci. USA *93*, 13780–13785.

Steimle, P. A., Yumura, S., Cote, G. P., Medley, Q. G., Polyakov, M. V., Leppert, B., and Egelhoff, T. T. (2001). Recruitment of a myosin heavy chain kinase to actin-rich protrusions in *Dictyostelium.* Curr. Biol. *11*, 708–713.

Stephens, L., Ellson, C., and Hawkins, P. (2002). Roles of PI3Ks in leukocyte chemotaxis and phagocytosis. Curr. Opin. Cell Biol. *14*, 203–213.

Sutoh, K. (1993). A transformation vector for *Dictyostelium discoideum* with a new selectable marker bsr. Plasmid *30*, 150–154.

Tuxworth, R. I., Cheetham, J. L., Machesky, L. M., Spiegelmann, G. B., Weeks, G., and Insall, R. H. (1997). *Dictyostelium* RasG is required for normal motility and cytokinesis, but not growth. J. Cell Biol. *138*, 605–614.

Van Haastert, P. J., and Devreotes, P. N. (2004). Chemotaxis: signalling the way forward. Nat. Rev. Mol. Cell. Biol. *5*, 626–634.

Washburn, M. P., Wolters, D., and Yates, J. R., III (2001). Large-scale analysis of the yeast proteome by multidimensional protein identification technology. Nat. Biotechnol. *19*, 242–247.

Weiner, O. D., Neilsen, P. O., Prestwich, G. D., Kirschner, M. W., Cantley, L. C., and Bourne, H. R. (2002). A PtdInsP(3)- and Rho GTPase-mediated positive feedback loop regulates neutrophil polarity. Nat. Cell Biol. *4*, 509–513.

Wessels, D., Soll, D. R., Knecht, D., Loomis, W. F., De Lozanne, A., and Spudich, J. (1988). Cell motility and chemotaxis in *Dictyostelium* amebae lacking myosin heavy chain. Dev. Biol. *128*, 164–177.

Wessels, D., Voss, E., Von Bergen, N., Burns, R., Stites, J., and Soll, D. R. (1998). A computer-assisted system for reconstructing and interpreting the dynamic three-dimensional relationships of the outer surface, nucleus and pseudopods of crawling cells. Cell Motil. Cytoskelet. *41*, 225–246.

Williams, M. R., Arthur, J. S., Balendran, A., van der Kaay, J., Poli, V., Cohen, P., and Alessi, D. R. (2000). The role of 3-phosphoinositide-dependent protein kinase 1 in activating AGC kinases defined in embryonic stem cells. Curr. Biol. *10*, 439–448.